Global Change Biology

Global Change Biology (2017) **23**, 2874–2886, doi: 10.1111/gcb.13590

Chlorophyll fluorescence tracks seasonal variations of photosynthesis from leaf to canopy in a temperate forest

HUALEI YANG[1,2], XI YANG[3,4], YONGGUANG ZHANG[5], MARY A. HESKEL[2], XIAOLIANG LU[2], J. WILLIAM MUNGER[6], SHUCUN SUN[1] and JIANWU TANG[2]

[1]*School of Life Sciences, Nanjing University, Jiangsu 210093, China,* [2]*Marine Biological Laboratory, The Ecosystems Center, Woods Hole, MA 02543, USA,* [3]*Department of Earth, Environmental and Planetary Sciences, Brown University, Providence, RI 02912, USA,* [4]*Department of Environmental Sciences, University of Virginia, Charlottesville, VA 22903, USA,* [5]*International Institute for Earth System Science, Nanjing University, Jiangsu 210093, China,* [6]*Department of Earth and Planetary Sciences, School of Engineering and Applied Sciences, Harvard University, Cambridge, MA, USA*

Abstract

Accurate estimation of terrestrial gross primary productivity (GPP) remains a challenge despite its importance in the global carbon cycle. Chlorophyll fluorescence (ChlF) has been recently adopted to understand photosynthesis and its response to the environment, particularly with remote sensing data. However, it remains unclear how ChlF and photosynthesis are linked at different spatial scales across the growing season. We examined seasonal relationships between ChlF and photosynthesis at the leaf, canopy, and ecosystem scales and explored how leaf-level ChlF was linked with canopy-scale solar-induced chlorophyll fluorescence (SIF) in a temperate deciduous forest at Harvard Forest, Massachusetts, USA. Our results show that ChlF captured the seasonal variations of photosynthesis with significant linear relationships between ChlF and photosynthesis across the growing season over different spatial scales (R^2 = 0.73, 0.77, and 0.86 at leaf, canopy, and satellite scales, respectively; $P < 0.0001$). We developed a model to estimate GPP from the tower-based measurement of SIF and leaf-level ChlF parameters. The estimation of GPP from this model agreed well with flux tower observations of GPP (R^2 = 0.68; $P < 0.0001$), demonstrating the potential of SIF for modeling GPP. At the leaf scale, we found that leaf F_q'/F_m', the fraction of absorbed photons that are used for photochemistry for a light-adapted measurement from a pulse amplitude modulation fluorometer, was the best leaf fluorescence parameter to correlate with canopy SIF yield (SIF/APAR, R^2 = 0.79; $P < 0.0001$). We also found that canopy SIF and SIF-derived GPP (GPP_{SIF}) were strongly correlated to leaf-level biochemistry and canopy structure, including chlorophyll content (R^2 = 0.65 for canopy GPP_{SIF} and chlorophyll content; $P < 0.0001$), leaf area index (LAI) (R^2 = 0.35 for canopy GPP_{SIF} and LAI; $P < 0.0001$), and normalized difference vegetation index (NDVI) (R^2 = 0.36 for canopy GPP_{SIF} and NDVI; $P < 0.0001$). Our results suggest that ChlF can be a powerful tool to track photosynthetic rates at leaf, canopy, and ecosystem scales.

Keywords: carbon cycle, chlorophyll, gross primary production, photosynthesis, solar-induced fluorescence, vegetation indices

Received 1 June 2016 and accepted 2 November 2016

Introduction

The total production of biomass with its chemical energy converted from sunlight energy via plant photosynthesis at the canopy scale, termed gross primary productivity (GPP), drives ecosystem function and carbon cycling. At the landscape level, GPP can be estimated from eddy covariance data as the difference between net ecosystem exchange (NEE) and the total ecosystem respiration, or from remotely sensed satellite products (Miura *et al.*, 2000; Heinsch *et al.*, 2006; Williams *et al.*, 2009; Zhao & Running, 2010; Frankenberg *et al.*, 2011; Jung *et al.*, 2011; Migliavacca *et al.*, 2011). However, direct measurement of GPP at the landscape or regional scale is not available. The Monteith (1972, 1977) model has been used to calculate GPP as a function of absorbed light energy (i.e., absorbed photosynthetically active radiation, APAR) multiplied by the light use efficiency (ε) that converts light energy to chemical energy stored as plant biomass (i.e., GPP=APAR*ε). Unfortunately, it is challenging to accurately estimate light use efficiency (ε) and APAR at large scales because these parameters may vary with different biomes, physiological factors, and environmental conditions (Medlyn, 1998; Frankenberg *et al.*, 2011). Therefore, there is a critical need to develop a more accurate method to estimate GPP and its temporal variation through seasons.

Correspondence: Jianwu Tang, tel. 1 508 289 7162, fax 508 457 1548, e-mail: jtang@mbl.edu

Light energy captured by the leaf chlorophyll molecules and transferred to the reaction centers is released via three different pathways, photochemistry, nonphotochemical quenching (NPQ, i.e., heat dissipation), and a small fraction re-emitted as chlorophyll fluorescence (ChlF). More recently, advancements in measurement techniques have found that ChlF detected at the canopy and landscape scales correlated with photosynthesis and/or GPP at those scales (Guanter *et al*., 2012, 2014; Lee *et al*., 2013; Yang *et al*., 2015).

Using fluorescence signals to derive leaf photosynthesis or canopy GPP at multiple scales has received increasing attention. At the leaf scale, many pulse amplitude modulation (PAM) fluorometers have been developed to simultaneously measure ChlF and photosynthetic CO_2 uptake (Bolhar-Nordenkampf *et al*., 1989; Rascher *et al*., 2000; Naumann *et al*., 2007; Galle *et al*., 2009; Van der Tol *et al*., 2014). The PAM fluorometers, which integrate a gas exchange system with a fluorescence chamber head, can accurately measure plant photosynthetic physiology *in vivo* (Long & Bernacchi, 2003). At the larger scale, using solar-induced chlorophyll fluorescence (SIF) signals over a narrow spectral region on remote sensing platforms (e.g., above-canopy towers, aircrafts, and satellites) has grown over the past decade to estimate GPP (Grace *et al*., 2007; Baker, 2008; Meroni *et al*., 2009; Rascher *et al*., 2009; Damm *et al*., 2010; Frankenberg *et al*., 2011; Joiner *et al*., 2011, 2012, 2013; Porcar-Castell *et al*., 2014). Currently, spectroradiometer systems that observe tower (canopy)-SIF signal based on the measurements of solar irradiance and vegetation radiance have recorded a strong relationship between SIF and GPP at the canopy scale (Rossini *et al*., 2010; Yang *et al*., 2015). At the global scale, satellite technologies have been developed to retrieve the regional SIF signal, for example, the Greenhouse Gases Observing Satellite (GOSAT) and Global Ozone Monitoring Experiment 2 (GOME-2) (Frankenberg *et al*., 2011; Joiner *et al*., 2011, 2013; Guanter *et al*., 2012). Joiner *et al.* (2013) demonstrated that the spatial and temporal variability in SIF derived from GOME-2 agreed with that of GOSAT-SIF. Satellite observation of terrestrial chlorophyll fluorescence could provide important information on plant growth status, the carbon balance of terrestrial ecosystems, and the length of the carbon uptake period (Guanter *et al*., 2014; Zhang *et al*., 2014; Lee *et al*., 2015). However, at present, little is known about the linkage between leaf-level ChlF and canopy-SIF.

In addition, the relationship between SIF and GPP is not fully understood. Some researchers reported that SIF exhibited a strong linear correlation with GPP on the global (Frankenberg *et al*., 2011; Guanter *et al*., 2012) and canopy level (Guanter *et al*., 2013; Yang *et al*., 2015). Others considered the relationship between SIF and GPP could not be strictly linear and the application of a linear relationship between SIF and GPP could introduce biases in the estimation of GPP (e.g., Lee *et al*., 2015).

In this study, we measured chlorophyll fluorescence and carbon exchange at both leaf and canopy scales at Harvard Forest, MA, USA, with the objective of more accurately characterizing the relationship between SIF and GPP. Our primary goals are (i) to investigate the seasonal dynamics of ChlF and photosynthesis and study their correlations at different spatial scales during the growing season; (ii) to explore the linkages between leaf-level ChlF parameters and the canopy- and satellite-level SIF; and (iii) to predict GPP from SIF measurements and compare the SIF-derived GPP with eddy covariance-based GPP.

Materials and methods

Site description

Chlorophyll fluorescence and gas exchange measurements on the leaf scale were conducted on a walk-up tower site, which is located at a hardwood stand at the Harvard Forest, Petersham, Massachusetts, USA (42°32′6″N, 72°10′28″W). The site is characterized with cool, moist temperate climate with average temperatures of −7°C in January and 20°C in July. The annual precipitation is averaged at 1100 mm, distributed evenly throughout the year. Snow typically covers the ground for several months during winter. The approximately 80–100 years old mixed hardwood stand is dominated by American beech (*Fagus grandifolia Ehrh.*), red oak (*Quercus rubra.*), and red maple (*Acer rubrum L.*). Soils are mainly sandy loam glacial till, with some alluvial and colluvial deposits. Photosynthetically active radiation (PAR) and air temperature data were collected from the walk-up tower. The canopy-level SIF data were collected from the nearby barn tower (Yang *et al*., 2015). An eddy covariance tower at the Environmental Monitoring site (EMS) measured CO_2 exchange and environmental data. These three locations are within 1.5 km from each other and covered by similar vegetation composition and soil types.

Chlorophyll fluorescence

We used a LI-6400XT with an integrated leaf chamber fluorometer (LCF) (LI-6400-40; LI-COR, Inc., Lincoln, NE, USA), a pulse amplitude modulation (PAM) system that has an LED-based fluorescence source accessory to simultaneously measure leaf-based chlorophyll fluorescence and photosynthesis rates. The rapid and nondestructive measurements of leaf chlorophyll fluorescence were conducted on randomly selected leaves from *Fagus grandifolia Ehrh.* and *Quercus rubra*. trees. We selected 3–5 leaves from each canopy heights (2, 7, 12, 17, and 23 m) at different time of the day (n = 90 per day) (daily in spring and autumn and monthly in summer) and used LI-6400XT *in situ*. We used light of different intensities on a dark-adapted and a light-adapted leaf to estimate fluorescence kinetics (i.e., the Kautsky curve) (Bradbury & Baker,

1981; Baker, 2008). When a leaf was placed in the dark for more than 30 min (Larcher & Cernusca, 1985), the PSII reaction centers were completely open (i.e., the primary quinone electron acceptor (QA) was oxidized). Then, the dark-adapted leaf was exposed to a weak red light (intensity was 3 μmol m^{-2} s^{-1}) with wavelength centered at 630 nm and the LCF detected the initial minimum fluorescence, termed F_o. Then, after the leaf was exposed to saturated flash lights (light intensity>7000 μmol m^{-2} s^{-1}), there was an immediate rise in fluorescence to an initial maximal level, termed F_m, representing that the PSII reaction centers were completely closed and fluorescence maximized. Another leaf was measured for the light-adapted process. With an actinic light provided by LCF at the intensity that was adjusted equivalent to the ambient light to drive photosynthesis, the fluorescence reached a stable state on 715-nm wavelength, termed F_s. The actinic light was turned off, and a weak far red light (the wavelength centered at about 740 nm with the intensity of 30 μmol m^{-2} s^{-1}) was emitted to measure minimal fluorescence of the light-adapted leaf, termed F_o'. The fluorescence rose to a maximum when the light-adapted leaf was exposed to a brief saturating flash (similar to that of the dark-adapted leaf), termed F_m'. Normally, F_o' is higher than F_o and F_m' is lower than F_m, as the reaction centers cannot completely open for F_o' or completely close for F_m' for the light-adapted leaf. Thus, the fluorescence parameters can be calculated by the following formulas:

$$F_v/F_m = \frac{F_m - F_o}{F_m} \quad (1)$$

where F_v/F_m means the fraction of absorbed photons that are used for photochemistry for a dark-adapted leaf, which usually reflects the potential photosynthetic capacity or photosynthetic efficiency of plants. F_o and F_m are the dark-adapted minimum and maximum fluorescence, respectively.

$$F_q'/F_m' = \frac{F_m' - F_s}{F_m'} \quad (2)$$

where F_q'/F_m' is the fraction of absorbed photons that are used for photochemistry for a light-adapted leaf (photochemical yield). F_s is the steady-state fluorescence, and F_m' is the maximal value under a saturating flash light. All the leaf-scale fluorescence parameters were averaged across leaves from different species and canopy locations as the daily mean values.

For the canopy fluorescence signal observation, we used a recently published technique (Yang *et al*., 2015) to continuously (at 5-min intervals) measure solar-induced fluorescence (SIF) from a spectrometric system from May to October, 2014. The spectrometer, capable of measuring spectra with a spectral resolution of ~0.13 nm between 680 and 760 nm (HR2000+, Ocean Optics, Inc., Dunedin, FL, USA), was connected to two fiber optic cables, one of which was pointed vertically toward the sky collecting total solar irradiance, and the other toward the target canopy (viewing zenith angle: 30°) measuring the vegetation radiance. The paired solar irradiance and vegetation radiance were recorded every 5 min and converted to valid data with the units of mWm^{-2} nm^{-1} and mWm^{-2} sr^{-1} nm^{-1} for irradiance and radiance, respectively, with radiometric calibration. Finally, we calculated the SIF at 760 nm from the irradiance and radiance observations under clear sky conditions (when diffuse radiation/(diffuse radiation + direct radiation) <0.5) using the spectral fitting methods (SFM) (Meroni *et al*., 2009; Yang *et al*., 2015). Daily mean SIF between 6:00 AM and 6:00 PM was calculated, and the outliers (due to overcast or machine error) were removed from subsequent graphs for clarity.

We used data from satellite GOME-2 (The Global Ozone Monitoring Experiment-2) level 2 products that provided SIF referenced to 740 nm (SIF_{740}) with ~0.5-nm spectral resolution (spatial resolution is 40 km × 80 km) (Joiner *et al*., 2013). Monthly SIF_{740} was extracted at the pixel covering Harvard Forest from May to October in 2014. To compare with the canopy SIF_{760}, GOME-2 SIF_{740} was converted to SIF_{760} by multiplying by a specific coefficient 0.582 (Yang *et al*., 2015). The monthly GOME-2 SIF_{760} time series data were smoothed using the Savitzky–Golay filter.

Gas exchange measurements

Leaf net photosynthetic rate (P_{net}, μmol m^{-2} s^{-1}) was quantified in parallel with the measurements of leaf fluorescence using an open gas exchange system (LI-6400XT; LI-COR, Inc.) under a imposed light intensity (i.e., PAR) according to the ambient radiance with a constant CO_2 level around 400 μmol m^{-2} s^{-1}, and during the plant growing season (Xu *et al*., 2008). We calculated leaf apparent photosynthesis ($P_{apparent}$) as dark respiration (P_{net} when PAR = 0) plus P_{net} at a given light intensity (Wohlfahrt & Gu, 2015). Our measurements did not include simultaneous estimates of photorespiration, thus limiting our ability to calculate true gross photosynthesis (Wohlfahrt & Gu, 2015). Daily mean $P_{apparent}$ was calculated as the average of the values across the leaves from different canopy layers over the course of a day. In addition, we measured light response curves of $P_{apparent}$ and F_q'/F_m'. The leaf was illuminated for 20–30 min until steady-state fluorescence and gas exchange values were recorded. The irradiances used for the light response curve were 50, 100, 300, 500, 800, 1200, and 1600 μmol m^{-2} s^{-1}.

Daily mean GPP at the canopy scale was calculated from data collected using the eddy covariance techniques. We applied REddyProcWeb online tool (http://www.bgc-jena.mpg.de/bgi/index.php/Services/REddyProcWeb) with the eddy covariance and meteorological data on EMS (Environmental Monitoring Station) tower at Harvard Forest and used the flux partitioning algorithms to partition net ecosystem (NEE) into GPP and ecosystem respiration (Reichstein *et al*., 2005; Yang *et al*., 2015). Daily mean GPP (GPP_{EC}) was calculated as the ratio of the sum of hourly GPP to the daytime length (PAR >0 μmol m^{-2} s^{-1}). Also, for the satellite-based GPP (GPP_{SAT}), 8-day 1-km Moderate Resolution Imaging Spectroradiometer (MODIS) GPP (MOD17A2) data of Harvard Forest (within approximately the same tower averaging area) in year 2014 were downloaded (http://modis-land.gsfc.nasa.gov/).

Leaf traits and vegetation indices

We used a Soil Plant Analysis Development (SPAD)-502 meter (Spectrum Technologies, Aurora, IL, USA) to monitor changes of chlorophyll concentration during the growing season. This nondestructive technique has been used to estimate leaf

chlorophyll concentration rapidly and accurately by measuring the leaf transmittance in two wavebands centered at 650 and 940 nm. We selected 15 sunlit leaves from the top of the canopy of the *Quercus rubra* and *Fagus grandifolia Ehrh.* each day and made five SPAD readings for each leaf that were evenly distributed over the whole leaf area. We found that there was no difference in SPAD values between *Quercus rubra* and *Fagus grandifolia Ehrh.* by *t*-tests in Excel with species as a factor ($t = 0.47$; $P = 0.64$); hence, average SPAD across leaves and the two species were made per day to calculate SPAD of the stand.

To estimate seasonality of vegetation development from spring leaf-out to autumn senescence, we used a tower-based Tetracam Agriculture Digital Camera (Tetracam, Inc., Chatsworth, CA, USA) during the growing season as a simple and accurate technique to monitor vegetation reflectance in visible and near-infrared bands to estimate canopy Normalized Difference Vegetation Index (NDVI). Leaf area index (LAI) of the forest was measured using a LAI-2000 Plant Canopy Analyzer (LI-COR, Inc.), when the sun was near the horizon (before sunrise or after sunset), or on overcast days to reduce the contribution of scattered radiation.

To investigate the independent effects of vegetation structure (LAI) and leaf physiology (chlorophyll) on SIF variability, a one-by-one sensitivity analysis was performed with the SCOPE model (Soil Canopy Observation of Photosynthesis and the Energy Balance) (Van der Tol *et al.*, 2009b) with the most informative leaf optical properties and canopy structural variables: maximum carboxylation capacity (Vcmo), leaf chlorophyll content (Cab), leaf inclination (LIDFa), incoming shortwave radiation (Rin), and leaf area index (LAI) (Zhang *et al.*, 2016).

Estimation of GPP using SIF

We calculated canopy GPP using measurements of SIF and extended the relationship between photosynthesis and fluorescence from the leaf scale to the canopy. As chlorophyll fluorescence (ChlF), here measured as canopy-scale SIF and leaf-scale F_s, is a by-product of the light reactions of photosynthesis, we can evaluate ChlF as the product of absorbed radiation and light use efficiency (Guanter *et al.*, 2014) in a similar way to photosynthesis expressed as light intensity and photosynthesis efficiency; that is, photosynthesis or fluorescence can be calculated as the product of absorbed light intensity and photosynthesis quantum efficiency (ε_P) or fluorescence quantum efficiency (ε_F) (Lee *et al.*, 2015):

At the leaf scale:

$$P_{apparent} = \mathrm{APAR_L} * \varepsilon_{\mathrm{PL}} \tag{3}$$

$$F_s = \mathrm{APAR_L} * \varepsilon_{\mathrm{FL}} \tag{4}$$

At the canopy scale:

$$\mathrm{GPP} = \mathrm{APAR_C} * \varepsilon_{\mathrm{PC}} \tag{5}$$

$$\mathrm{SIF} = \mathrm{APAR_C} * \varepsilon_{\mathrm{FC}} \tag{6}$$

where $\varepsilon_{\mathrm{PL}}$ and $\varepsilon_{\mathrm{FL}}$ are photosynthesis quantum efficiency and fluorescence quantum efficiency, respectively, at the leaf scale, and $\varepsilon_{\mathrm{PC}}$ and $\varepsilon_{\mathrm{FC}}$ are photosynthesis quantum efficiency and fluorescence quantum efficiency, respectively, at the canopy scale. $\mathrm{APAR_L}$ is the absorbed photosynthetically active radiation (μmol m^{-2} s^{-1}) at the leaf scale and can be calculated as $\mathrm{APAR_L} = \mathrm{PAR} * f * \alpha_{\mathrm{leaf}}$. PAR refers to the imposed photosynthetically active radiation (μmol m^{-2} s^{-1}) from LiCor 6400-LCF, f is the fraction of absorbed photons that are used by PS II (usually is 0.5 for C3 plants), and α_{leaf} means leaf absorptivity and is typically estimated to 0.84 (Genty *et al.*, 1989). $\mathrm{APAR_C}$ is the absorbed photosynthetically active radiation (μmol m^{-2} s^{-1}) at the canopy scale and can be calculated as $\mathrm{APAR_c} = \mathrm{PAR_{up}}\text{-}\mathrm{PAR_{reflect}}\text{-}\mathrm{PAR_{under}}$ (Yang *et al.*, 2015). $\mathrm{PAR_{up}}$, $\mathrm{PAR_{reflect}}$, and $\mathrm{PAR_{under}}$ are solar incident PAR, reflected PAR from canopy, and lower-canopy incident PAR, respectively.

Both F_s and SIF refer to the light-adapted steady-state fluorescence value. Measured F_s is a relative, unitless value and cannot be directly compared to SIF. So, we provide a correction coefficient (c) to represent actual F_s (i.e., $c*F_s$ for corrected F_s). Here, c is an instrument-specific constant, calculated as below (Eqn 9).

The PAR conversion efficiency (ε) can be parameterized as a function of meteorological parameters and varies with different vegetation types (Field *et al.*, 1995; Prince & Goward, 1995; Turner *et al.*, 2003). We assumed the value of leaf scale $\varepsilon_{\mathrm{PL}}$ or $\varepsilon_{\mathrm{FL}}$ across leaves from different canopy layers represents the canopy-scale $\varepsilon_{\mathrm{PC}}$ or $\varepsilon_{\mathrm{FC}}$ (Middleton *et al.*, 2009), that is, $\varepsilon_{\mathrm{PL}} = \varepsilon_{\mathrm{PC}}$, $\varepsilon_{\mathrm{FL}} = \varepsilon_{\mathrm{FC}}$. Therefore,

$$\frac{P_{apparent}}{\mathrm{APAR_L}} = \frac{\mathrm{GPP}}{\mathrm{APAR_C}} \tag{7}$$

$$\frac{\mathrm{c} * F_s}{\mathrm{APAR_L}} = \frac{\mathrm{SIF}}{\mathrm{APAR_C}} \tag{8}$$

Under a given incident light (for example, PAR = 600 μmol m^{-2} s^{-1}) on leaf and canopy scales, the correction coefficient (c) can be calculated from Eqn (9):

$$c = \frac{\mathrm{APAR_L}}{\mathrm{APAR_C}} * \frac{\mathrm{SIF}}{F_s} \tag{9}$$

Using the measured values during the growing season, c values were found to be relatively stable around 0.0001; therefore, c value was typically assumed as 0.0001(mW m^{-2} sr^{-1} nm^{-1} per F_s count) in this study (S1).

From Eqns (7) and (8), we derive a relationship between GPP and SIF:

$$\mathrm{GPP} = (P_{apparent}/(c{*}F_s)) * \mathrm{SIF} \quad \text{or} \tag{10}$$

$$\mathrm{GPP/SIF} = P_{apparent}/(c * F_s) \tag{11}$$

Equations (10) and (11) show that GPP at the canopy scale can be calculated from SIF measurements, given the known leaf-scale parameter, $P_{apparent}$ /($c*F_s$). Thus, estimated GPP from SIF can be independently compared with the eddy covariance-based GPP and satellite-based GPP.

Results

The seasonality of leaf chlorophyll fluorescence and photosynthesis parameters over different spatial scales

Seasonal patterns of leaf chlorophyll fluorescence and photosynthesis were observed at the leaf, canopy, and

satellite levels (Fig. 1). According to the previous study on the seasonality of the vegetation indices and plant physiological traits based on the NDVI (Normalized Difference Vegetation Index) measured by an NDVI camera and leaf chlorophyll concentration at this site, we identified spring (DOY 132-167), summer (DOY 168-260), and autumn (DOY 261-311) (Yang *et al*., 2016).

On the leaf scale, the ChlF parameters (F_s, F_v/F_m, F_q'/F_m') and photosynthetic rate ($P_{apparent}$) increased after leaf emergence and reached to summer peak around DOY 168 (for example, F_s and $P_{apparent}$ increased 70%). In autumn, F_q'/F_m' and $P_{apparent}$ decreased from late September (DOY 261) due to the leaf aging, and the decline appeared earlier (~10 days) than other leaf ChlF parameters (F_s, F_v/F_m). On the canopy scale, similar seasonality trajectories appeared among SIF, GPP_{SIF}, and GPP_{EC} over the growing season. In the seasonal cycle, onset of canopy-SIF and its derived GPP (GPP_{SIF}) appeared on DOY 127, a week earlier compared to GPP_{EC} (eddy flux GPP) after leaf emergence at the beginning of May. SIF, GPP_{SIF}, and GPP_{EC} had a rapid increase with green-up in spring until late June (approximately DOY 167) and reached its maximum around the middle summer, then sharply decreased from mid-September (~DOY 260) in the autumn due to leaf senescence and aging until dormancy period. For the satellite fluorescence and photosynthesis data, smoothed GOME-2 SIF and MODIS-GPP showed more fluctuation than SIF and GPP measured at the canopy scale, because of its coarse spatial and temporal resolution. Both GOME-2 SIF and MODIS-GPP increased in the spring season and reached the summer peak on DOY 167, and then declined slightly during the late summer season and rapidly in autumn starting DOY 265.

In general, the seasonal changes of ChlF appeared roughly synchronous with that of photosynthesis in leaf, canopy, and satellite scales. Furthermore, the spring rising points and autumn decline points of ChlF and photosynthesis parameters appeared earlier on the canopy and satellite scale than leaf level. ChlF and photosynthesis at all scales reached summer peak around DOY 167. Overall, the ChlF values were higher in spring than those in fall.

Leaf fluorescence parameters correlated with canopy SIF and GOME-2 SIF (Fig. 2). Strong correlations existed between F_q'/F_m' (indicating quantum yield of PS II at the leaf scale under a light condition) and canopy SIF (spring $R^2 = 0.64$, fall $R^2 = 0.75$), and between F_q'/F_m' and GOME-2 SIF (spring $R^2 = 0.64$, fall $R^2 = 0.77$), with all regressions highly significant ($P < 0.0001$). We also found that leaf-level ChlF and canopy SIF (or GOME-2 SIF) showed different slopes for spring and fall.

We examined the correlations between F_q'/F_m' (photochemical yield) and canopy-SIF/APAR (SIF yield) and found that the SIF yield was linearly increasing with photochemical yield under high-light conditions (Fig. 3), which is generally the overpass time of satellite observations of SIF.

Correlations between plant chlorophyll fluorescence and photosynthesis

There were significant seasonal relationships between ChlF and photosynthesis from leaf to satellite scales, explained by the gradual spring increases and autumn decreases in deciduous forest. At the leaf scale, the fluorescence parameter F_q'/F_m' was strongly linked to $P_{apparent}$ ($R^2 = 0.76$, 0.82 and 0.49 for spring, fall, and entire growing season, respectively; $P < 0.0001$), and F_s was highly related to $P_{apparent}$ ($R^2 = 0.70$, 0.82 and 0.73 for spring, fall, and entire growing season, respectively; $P < 0.0001$) (Fig. 4a, b). F_q'/F_m' had a declining light response curve, in contrast to that of $P_{apparent}$ (Fig. 5). Photosynthesis is a photobiochemical reaction process, and $P_{apparent}$ will accelerate rapidly with an increase of light intensity, but beyond a certain range (800–1200 μmol m^{-2} s^{-1}), $P_{apparent}$ increases slowly until it is saturated. On the contrary, with the increasing light intensity, F_q'/F_m' declined gradually and became saturation approximately under 1000 μmol m^{-2} s^{-1} light condition (Fig. 5).

At the canopy scale, SIF demonstrated a similar seasonal trend to GPP. Canopy-level SIF was positively correlated with GPP_{EC} ($R^2 = 0.75$ 0.69 and 0.77 in spring, fall, and entire growing season, respectively; $P < 0.0001$) (Fig. 4c). Similarly, on satellite scales, GOME-2 SIF was positively related to MODIS-GPP with the high correlation coefficients ($R^2 = 0.77$, 0.96, and 0.86 in spring, fall, and entire growing season, respectively; $P < 0.0001$) (Fig. 4d).

Estimating GPP using SIF based on leaf-scaled physiological properties

After comparing SIF-derived GPP (GPP_{SIF}) and eddy covariance tower-based GPP (GPP_{EC}) at the canopy scale, we found that GPP_{SIF} and GPP_{EC} had similar seasonal dynamics during the growing season that could be associated with phenological process in the deciduous forest (Fig. 1). The one-to-one regression results indicated that GPP_{SIF} was 1.0794 times of GPP_{EC} ($R^2 = 0.68$; $P < 0.0001$; RMSE = 4.0) (Fig. 6).

SIF-derived GPP correlated with chlorophyll content and vegetation indices

Remotely sensed SIF as well as SIF-derived GPP can reflect vegetation phenological pattern and relate to the

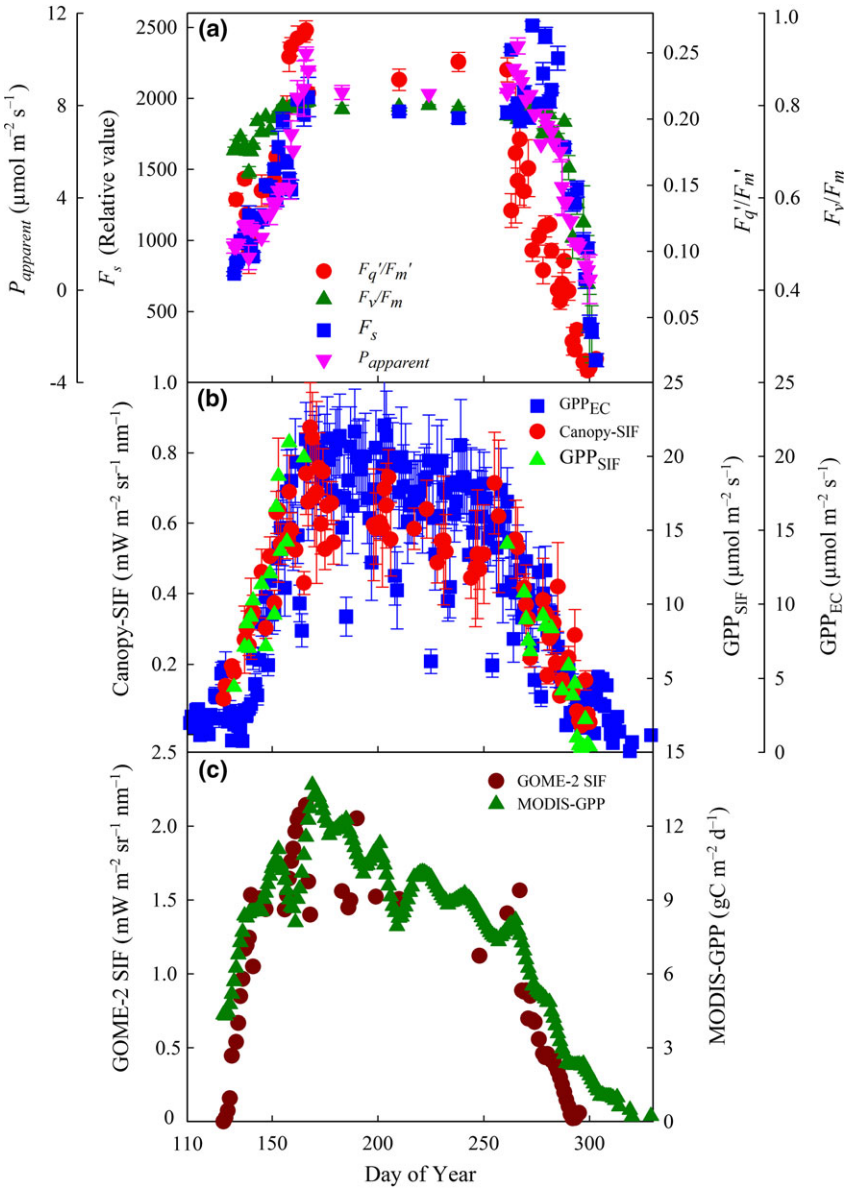

Fig. 1 The seasonality of leaf chlorophyll fluorescence and photosynthesis over different spatial scales. (a) Leaf-scaled chlorophyll fluorescence parameters: steady-state fluorescence (F_s), photochemistry efficiency of dark-adapted leaf (F_v/F_m), photochemistry efficiency of light-adapted leaf (F_q'/F_m'), leaf apparent photosynthesis ($P_{apparent}$); (b) canopy-scaled solar-induced fluorescence (SIF) and it derived gross primary productivity (GPP$_{SIF}$), and eddy covariance tower-based GPP (GPP$_{EC}$); (c) smoothed GOME-2 SIF and MODIS-GPP. The error bars are ± 1SE. [Colour figure can be viewed at wileyonlinelibrary.com].

biochemical (chlorophyll content) and structural (NDVI and LAI) parameters of the plants. Our results showed that SIF-derived GPP highly related with leaf chlorophyll content (R^2 = 0.65; P < 0.0001) (Fig. 7a). Concerning the relationships between GPP$_{SIF}$ and other vegetation indices that are typically linked to seasonal morphological development of plant canopies, both LAI and NDVI were significantly related to the seasonal dynamics of GPP$_{SIF}$ (R^2 = 0.35 between GPP$_{SIF}$ and LAI; R^2 = 0.36 between GPP$_{SIF}$ and NDVI; P < 0.0001) (Fig. 7b, c).

Figure 8 shows the independent influence of LAI and leaf chlorophyll content (Cab) on SIF variability. On the one hand, when LAI was fixed, SCOPE-SIF$_{760}$ increased with increased Cab and reached saturation at the point that Cab was around 25 μg cm^{-2} (Fig. 8a). On the other hand, SCOPE-SIF$_{760}$ increased with increasing canopy-LAI, and the rising curves between SCOPE-SIF$_{760}$ and LAI under Cab = 40 and Cab = 60 were very close with each other (Fig. 8b).

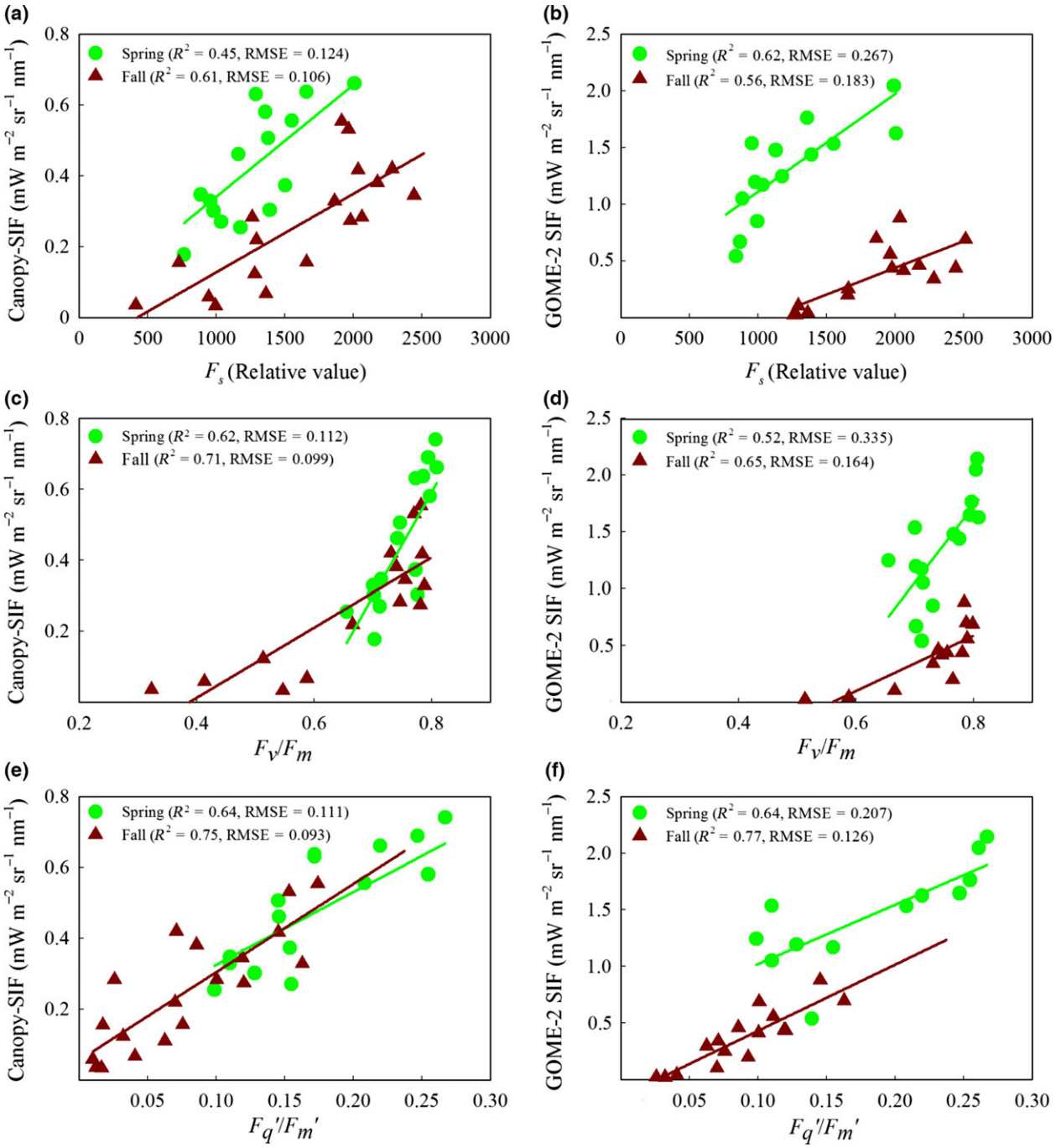

Fig. 2 The seasonal relationships between daily mean leaf-scaled fluorescence parameters and upscaled SIF. (a, b) Linear relationships between leaf-scaled steady-state fluorescence (F_s) and canopy-SIF and GOME-2 SIF, respectively; (c, d) linear relationships between leaf-scaled F_v/F_m and canopy-SIF and GOME-2 SIF, respectively; (e, f) linear relationships between leaf-scaled F_q'/F_m' and canopy-SIF and GOME-2 SIF, respectively. [Colour figure can be viewed at wileyonlinelibrary.com].

Discussion

In this study, we investigated the relationships between leaf-level ChlF parameters and canopy- or satellite-SIF, and the correlations between ChlF and plant photosynthetic capacity over multiple spatial scales.

The linkages between leaf and canopy fluorescence

We measured ChlF parameters from leaf to canopy and satellite scales. At the leaf level, the F_v/F_m represents the maximal quantum yield used for photochemistry (Kitajima & Butler, 1975). All green leaves that we

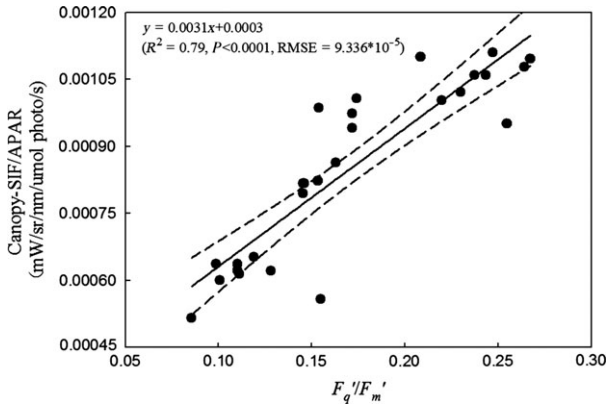

Fig. 3 The correlation between photochemical yield (*Fq′/Fm′*) and SIF yield (canopy-SIF/APAR) under 500–1000 μmol m^{-2} s^{-1} light intensity. The dotted lines represent 95% confidence interval. Coupled *Fq′/Fm′* and canopy-SIF/APAR were selected under the same light condition.

measured were typically in the range of 0.75–0.85, consistent with previous results (Flexas *et al.*, 2002). In unstressed environmental conditions, with increasing light intensity, the fraction of light energy used for photochemistry decreases and the fraction of light energy used for fluorescence increases (Seaton & Walker, 1990; Maxwell & Johnson, 2000; Van der Tol *et al.*, 2009a). F_q'/F_m' decreased in high-light conditions because of increases in nonphotochemical quenching (NPQ, i.e., heat dissipation), that reflecting a plant protection mechanism to avoid overenergization of the thylakoid membranes (Baker, 2008).

F_v/F_m and F_q'/F_m' are sensitive to physiological and environmental changes that affect the ability to capture light energy by open PSII reaction centers. F_q'/F_m' and CO_2 fixation capacity ($P_{apparent}$) showed greater difference in slopes for the spring and fall correlations than that between F_s and $P_{apparent}$ (Fig. 4a, b). With increased

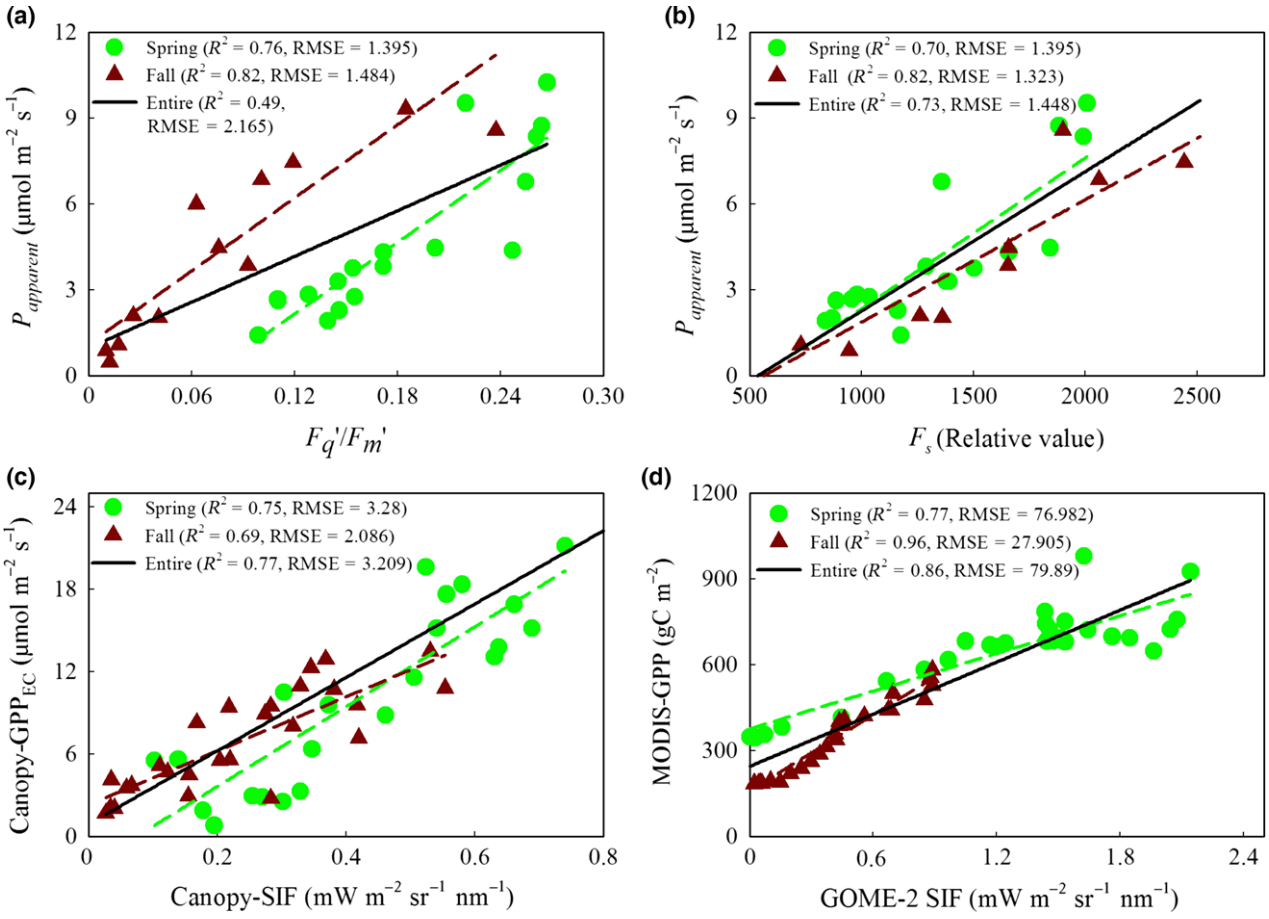

Fig. 4 The correlations between daily mean chlorophyll fluorescence and photosynthesis over different spatial scales. (a) Linear regressions between photochemistry efficient (F_q'/F_m') and apparent photosynthetic rate ($P_{apparent}$); (b) linear regressions between steady-state fluorescence (F_s) and $P_{apparent}$; (c) linear regressions between canopy-SIF and eddy covariance GPP; (d) linear regressions between GOME-2 SIF and MODIS-GPP. [Colour figure can be viewed at wileyonlinelibrary.com].

light intensity, the carbon fixation rate gradually increased and became light saturated, along with a decrease in photochemistry yield (i.e., F_q'/F_m') (Fig. 5) (Porcar-Castell *et al.*, 2014).

Leaf-scale ChlF parameters showed seasonally dependent correlations with SIF (canopy-SIF and GOME-2 SIF), and the slopes of the linear regressions were different for spring and autumn. F_v/F_m, which means maximum photosynthetic capacity, is usually stable for a healthy leaf, so the decline of F_v/F_m and the concurrently decline of canopy SIF (Fig. 2c) may directly prove that SIF could track photosynthetic capacity.

Also, we found that F_q'/F_m' showed better agreement with canopy-scale SIF than other leaf-scaled fluorescence parameters (F_s, F_v/F_m) (Fig. 2), indicating that F_q'/F_m', which involved leaf steady fluorescence (F_s) and actual maximal fluorescence (F_m'), was the best leaf-scale fluorescence parameter to interpret the upscaled fluorescence level. This consistency between F_q'/F_m' and canopy-SIF may be due to both of them indicating the information of electron transport rate (ETR) (Baker, 2008); in other words, canopy-SIF could capture leaf-level variations of ETR. This also

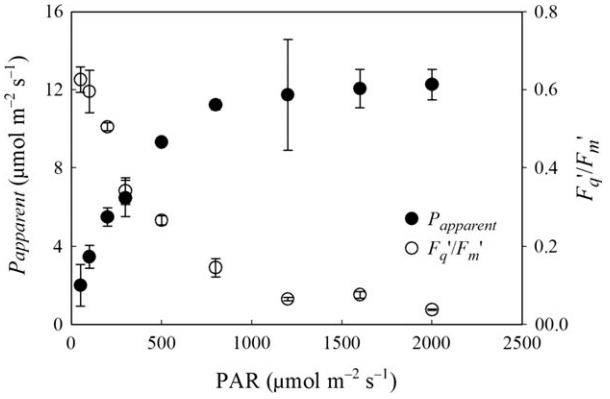

Fig. 5 The light response curves of F_q'/F_m' and $P_{apparent}$. The error bars are ± 1SE.

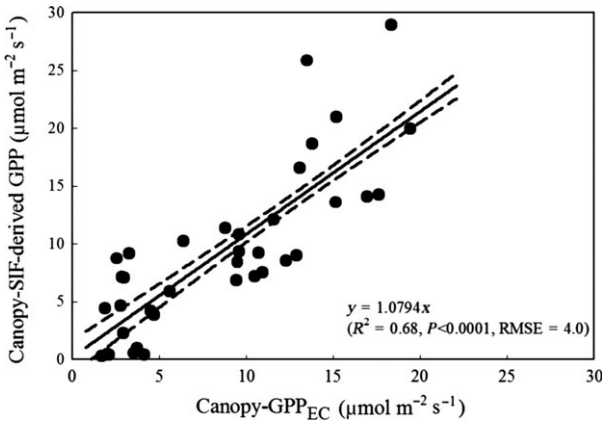

Fig. 6 The linear correlation between canopy GPP_{EC} and SIF-derived GPP (GPP_{SIF}) over 2014 growing season. The dotted lines represent 95% confidence interval.

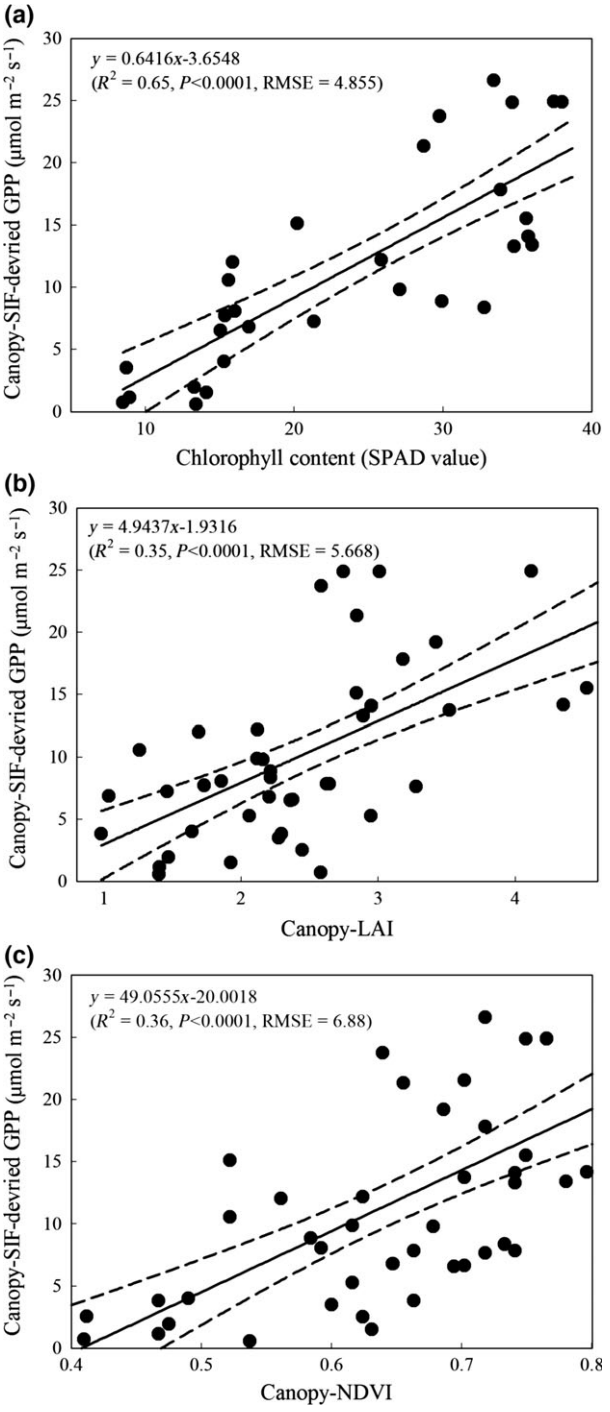

Fig. 7 SIF-derived GPP_{SIF} was significantly related to plant physiological and functional characteristics. The dotted lines represent 95% confidence interval.

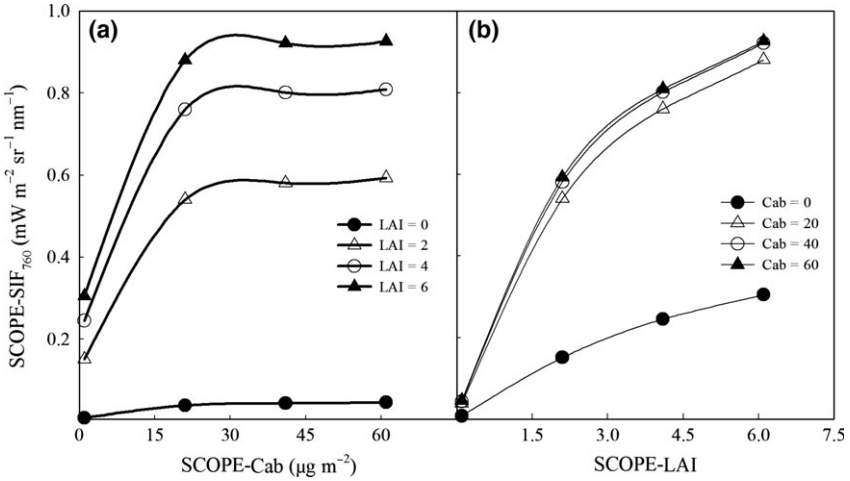

Fig. 8 The independent influence of leaf chlorophyll content (Cab) and LAI on SIF variability by fixing the maximum carboxylation capacity (Vcmo), incoming shortwave radiation (Rin), leaf inclination (LIDFa) as 100 μmol m^{-2} s^{-1}, 800Wm^{-2}, −1, respectively. All the values are simulated by SCOPE model.

supported the simulations by Guan *et al.* (2016) in which they showed the linear relationship between ETR and SIF for several crops. Furthermore, there was a significant, positive relationship between photochemical yield (F_q'/F_m') and SIF yield (canopy-SIF/APAR) under high-light conditions (Fig. 3), as both of photochemical yield and SIF yield decreased with increasing NPQ (Lee *et al.*, 2015). This finding from the field measurement supports the previous modeling result at canopy level (Lee *et al.*, 2015; Guan *et al.*, 2016).

The correlations between photosynthesis and fluorescence over different spatial scales

ChlF showed obvious seasonal variations with leaf spring development and autumn senescence. Photosynthesis had similar seasonal patterns to ChlF parameters (Fig. 1) across the season. Moreover, our results showed significant linear correlations between ChlF and photosynthesis on different spatial scales ($R^2 = 0.73$ between F_s and $P_{apparent}$, 0.77 between canopy-SIF and GPP_{EC}, 0.86 between GOME-2 SIF and MODIS-GPP for the entire growing season) for this deciduous forest (Fig. 4c, d), which suggested that SIF may better capture the seasonal change of GPP (carbon flux) in temperate deciduous forest ecosystems compared to existing models (e.g., GPP=APAR* ε) and satellite data products.

Simultaneously measured leaf-based ChlF and $P_{apparent}$ values are needed to link canopy SIF with GPP, with estimated $P_{apparent}/F_s$ as the leaf-level physiological basis of the model in place of the fixed ratio of GPP/SIF. The major assumptions of this model were (i) that both fluorescence and photosynthesis can be calculated as a product of absorbed radiance and light conversion efficiency across different spatial scales and (ii) that the mean value of ε_L from different canopy layers equals integrated canopy ε_C. It should be noted that the second assumption may slightly overestimate the low canopy's contributions to integrated canopy fluorescence and photosynthesis capacities, as the upper canopy should contribute more to the whole forest canopy although ε of upper canopy leaves may be limited by photoinhibition under high-light condition (Niinemets & Kull, 2001). However, our leaf samples involved sunlit, shaded, sunlit-shaded foliage from different canopy layers. So, the average of leaf scale ε should be close to the integrated ecosystem ε (Middleton *et al.*, 2009). This model eliminated the estimation of APAR, which relates to leaf physiology and canopy structure, based on the assumption that the average value of ε_L from different canopy levels can represent the whole canopy ε_C. Estimating APAR from NDVI may lead to a relatively inaccurate GPP value due to noise and errors in measuring NDVI, especially from satellite products (Yuan *et al.*, 2007). The significant relationship between GPP_{SIF} and GPP_{EC} (the slope of linear relationship between GPP_{SIF} and GPP_{EC} was close to 1 with the intercept as 0; Fig. 6) supports the feasibility of the model (Eqn 10), indicating that SIF may provide an additional approach to estimate the seasonality of photosynthesis for the deciduous forest. However, the points with high GPP_{SIF} value (GPP_{SIF}>25 μmol m^{-2} s^{-1}) were seriously deviated from the modeled line, which may be caused by the high $P_{apparent}$ values measured on those two days (with relatively high air temperature and low humidity). Therefore, we should be cautious about the maximum

values of GPP_{SIF} and GPP_{EC}. In addition, the significant linear relationships between leaf-level ChlF and $P_{apparent}$ when measured under the same conditions confirm the correlation between SIF and GPP values at larger scale that were obtained from different monitoring sensors.

The correction coefficient, c, is important for the calculation of $F_{s,}$ which was assumed as an instrument-specific constant representing the real meaning of leaf-scaled fluorescence values measured by LI-6400 fluorometer. The uncertainties in c are due to $APAR_L$, $APAR_C$, canopy-SIF, and leaf-F_s. Leaf-F_s was measured at a central wavelength of 710 nm (the range is between 700 and 715 nm), but canopy-SIF was measured at 760-nm wavelength including both PSI and PSII fluorescence signals. Thus, PAM fluorescence included fluorescence information in the wavelength that was not measured by canopy-SIF, and canopy SIF may be influenced by PSI fluorescence that was very low (in contrast to PSII) and constant under light (Porcar-Castell *et al*., 2014). It should also be mentioned that the radiometric unit of SIF is useful for scaling or comparing to other ecosystems (e.g., Eqn 9), as SIF is based on spectral measurements of radiometrically calibrated radiances (solar irradiance and vegetation radiance). In the future, it would be useful to measure solar-induced components of fluorescence to capture both downward and upload signals form leaves (Wittenberghe *et al*., 2015).

SIF and SIF-derived GPP correlate with chlorophyll content and other traits

SIF and its derived GPP show a strong seasonal pattern that is affected by seasonal variation in canopy chlorophyll content (Wittenberghe *et al*., 2013; Gitelson & Gamon, 2015). In spring, leaf fluorescence and photosynthesis generally increase with the increasing chlorophyll content after green-up; while in autumn, leaf fluorescence and the photosynthetic rate reduced associated with leaf physiological properties, especially in chlorophyll content, with declining with leaf aging and senescence (Fig. 7a) (David *et al*., 1998). Over the growing season, SIF-derived GPP show the significant correlations with vegetation greenness index (NDVI) and canopy structural parameter (LAI) (R^2 = 0.35 between GPP_{SIF} and LAI; R^2 = 0.36 between GPP_{SIF} and NDVI; $P < 0.0001$) (Fig. 7b, c), which are widely used to monitor the seasonal changes of terrestrial ecosystems that represent the growing season length and carbon uptake period (Baret *et al*., 2007; Zarco-Tejada *et al*., 2013). Therefore, ChlF can be a powerful and sensitive tool to monitor the seasonal cycle of photosynthetic activity for deciduous vegetation (Campbell *et al*., 2008; Rohacek *et al*., 2008).

Furthermore, our SCOPE simulation stated the independent influence of leaf chlorophyll content and vegetation structure on SIF variability for unstressed C3 canopy. Figure 8 revealed that the SIF_{760} remained increasing with LAI as more leaves emit more SIF_{760}, and the growth rate of SIF_{760} became slower under high LAI probably due to little light penetrated through the upper canopy and absorbed by lower canopy within a high-density canopy (Verrelst *et al*., 2015; Zhang *et al*., 2016). However, chlorophyll content (Cab) had more complex effects on SIF_{760}. At the initial stage of Cab development, SIF_{760} increased with Cab, whereas SIF_{760} became saturated at the high chlorophyll contents due to the saturation of light absorption by chlorophyll molecules at the high chlorophyll contents (Porcar-Castell *et al*., 2014). Zhang *et al.* (2016) have evaluated the SCOPE models with field measurements of SIF at Harvard Forest and showed that the models were generally consistent with the field measurements.

In summary, our study links leaf-level fluorescence with canopy-level SIF and reveals the correlations between fluorescence and photosynthesis over different spatial scales. The linear relationships between ChlF and photosynthesis during the growing season of canopy reflected that ChlF observations provide a powerful proxy to estimate global C budget. Moreover, sensitivity of ChlF signals provides a useful tool to understand the dynamic processes of vegetation growth in terrestrial ecosystems. We presented a model to estimate GPP, with the goal of tracking seasonal variation of GPP using tower-based SIF data in conjunction with concurrently measured leaf steady-state ChlF and photosynthesis. The estimated GPP_{SIF} is comparable with the measured GPP_{EC}. The physiological information provided by the PAM fluorescence measurements at the leaf scale may provide a pathway to better understand and establish the relationship between ChlF, electron transport, and photosynthesis across leaves and canopies.

Acknowledgements

We would like to thank Harvard Forest for providing site and logistic support during our research. This research was supported by U.S. Department of Energy Office of Biological and Environmental Research Grant DE-SC0006951, National Science Foundation Grants DBI-959333 and AGS-1005663, and the University of Chicago and the MBL Lillie Research Innovation Award to J. Tang, National Science Foundation of China Grants (41671421) to Y. Zhang, and China Scholarship Council (CSC) to H. Yang.

References

Baker NR (2008) Chlorophyll fluorescence: a probe of photosynthesis in vivo. *Annual Review of Plant Biology*, **59**, 659–668.

Baret F, Hagolle O, Geiger B *et al.* (2007) LAI, fAPAR and fCover CYCLOPES global products derived from VEGETATION. *Remote Sensing of Environment*, **110**, 275–286.

Bolhar-Nordenkampf HR, Long SP, Baker NR, Oquist G, Schreiber U, Lechner EG (1989) Chlorophyll fluorescence as a probe of the photosynthetic competence of leaves in the field: a review of current instrumentation. *Functional Ecology*, **3**, 497–514.

Bradbury M, Baker NR (1981) Analysis of the slow phases of the in vivo chlorophyll fluorescence induction curve. Changes in the redox state of photosystem II electron acceptors and fluorescence emission from photosystems I and II. *Biochimica et Biophysica Acta*, **635**, 542–551.

Campbell PKE, Middleton EM, Corp LA, Kim MS (2008) Contribution of chlorophyll fluorescence to the apparent vegetation reflectance. *Science of the Total Environment*, **404**, 433–439.

Damm A, Elbers J, Erler A *et al.* (2010) Remote sensing of sun-induced fluorescence to improve modeling of diurnal courses of gross primary production (GPP). *Global Change Biology*, **16**, 171–186.

David MM, Coelho D, Barrote I, Correia MJ (1998) Leaf age effects on photosynthetic activity and sugar accumulation in droughted and rewatered *Lupinus albus* plants. *Australian Journal of Plant Physiology*, **25**, 299–306.

Field CB, Randerson JT, Malmström CM (1995) Global net primary production: combining ecology and remote sensing. *Remote Sensing of Environment*, **51**, 74–88.

Flexas J, Escalona JM, Evain S, Gulıas J, Moya I, Osmond CB, Medrano H (2002) Steady-state chlorophyll fluorescence (Fs) measurements as a tool to follow variations of net CO_2 assimilation and stomatal conductance during water-stress in C_3 plants. *Physiologia Plantarum*, **114**, 231–240.

Frankenberg C, Fisher JB, Worden J *et al.* (2011) New global observations of the terrestrial carbon cycle from GOSAT: patterns of plant fluorescence with gross primary productivity. *Geophysical Research Letters*, **38**, 351–365.

Galle A, Florez-Sarasa I, Tomas M, Pou A, Medrano H, Ribas-Carbo M, Flexas J (2009) The role of mesophyll conductance during water stress and recovery in tobacco (*Nicotiana sylvestris*): acclimation or limitation? *Journal of Experimental Botany*, **60**, 2379–2390.

Genty B, Briantais JM, Baker NR (1989) The relationship between the quantum yield of photosynthetic electron transport and quenching of chlorophyll fluorescence. *Biochimica et Biophysica Acta*, **990**, 87–92.

Gitelson AA, Gamon JA (2015) The need for a common basis for defining light-use efficiency: implications for productivity estimation. *Remote Sensing of Environment*, **156**, 196–201.

Grace J, Nichol C, Disney M, Lewis P, Quaife T, Bowyer P (2007) Can we measure terrestrial photosynthesis from space directly, using spectral reflectance and fluorescence? *Global Change Biology*, **13**, 1484–1497.

Guan K, Berry JA, Zhang Y, Joiner J, Guanter L, Badgley G, Lobell DB (2016) Improving the monitoring of crop productivity using spaceborne solar-induced fluorescence. *Global Change Biology*, **22**, 716–726.

Guanter L, Dudhia A, Lewis PE, Gómez-Dans J, Kuze A, Suto H, Grainger RG (2012) Retrieval and global assessment of terrestrial chlorophyll fluorescence from GOSAT space measurements. *Remote Sensing of Environment*, **121**, 236–251.

Guanter L, Rossini M, Colombo R, Meroni M, Frankenberg C, Lee JE, Joiner J (2013) Using field spectroscopy to assess the potential of statistical approaches for the retrieval of sun-induced chlorophyll fluorescence from ground and space. *Remote Sensing of Environment*, **133**, 52–61.

Guanter L, Zhang Y, Jung M *et al.* (2014) Global and time-resolved monitoring of crop photosynthesis with chlorophyll fluorescence. *Proceedings of the National Academy of Sciences*, **111**, E1327–E1333.

Heinsch FA, Zhao M, Running SW *et al.* (2006) Evaluation of remote sensing based terrestrial productivity from MODIS using regional tower eddy flux network observations. *IEEE Transactions on Geoscience and Remote Sensing*, **44**, 1908–1925.

Joiner J, Yoshida Y, Vasilkov AP, Yoshida Y, Corp LA, Middleton EM (2011) First observations of global and seasonal terrestrial chlorophyll fluorescence from space. *Biogeosciences*, **8**, 637–651.

Joiner J, Yoshida Y, Vasilkov AP *et al.* (2012) Filling-in of near-infrared solar lines by terrestrial fluorescence and other geophysical effects: simulations and space-based observations from SCIAMACHY and GOSAT. *Atmospheric Measurement Techniques*, **5**, 809–829.

Joiner J, Guanter L, Lindstrot R *et al.* (2013) Global monitoring of terrestrial chlorophyll fluorescence from moderate-spectral-resolution near-infrared satellite measurements: methodology, simulations, and application to GOME-2. *Atmospheric Measurement Techniques*, **6**, 2803–2823.

Jung M, Reichstein M, Margolis HA *et al.* (2011) Global patterns of land-atmosphere fluxes of carbon dioxide, latent heat, and sensible heat derived from eddy covariance, satellite, and meteorological observations. *Journal of Geophysical Research*, **116**, G00J07.

Kitajima M, Butler WL (1975) Quenching of chlorophyll fluorescence and primary photochemistry in chloroplasts by dibromo-thymoquinone. *Biochimica et Biophysica Acta*, **76**, 105–115.

Larcher MW, Cernusca A (1985) Mikrocomputergesteuerte mobile Anlage zum fluoro-metrischen Nachweis von Photosynthesestörungen. *Sitzungsber österr Akad Wiss Math-Naturwiss K*, **194**, 45–64.

Lee JE, Frankenberg C, van der Tol C *et al.* (2013) Forest productivity and water stress in Amazonia: observations from GOSAT chlorophyll fluorescence. *Proceedings of the Royal Society B: Biological Sciences*, **280**, 176–188.

Lee JE, Berry JA, Van der Tol C *et al.* (2015) Simulations of chlorophyll fluorescence incorporated into the Community Land Model version 4. *Global Change Biology*, **21**, 3469–3477.

Long SP, Bernacchi CJ (2003) Gas exchange measurements, what can they tell us about the underlying limitations to photosynthesis? Procedures and sources of error. *Journal of Experimental Botany*, **54**, 2393–2401.

Maxwell K, Johnson GN (2000) Chlorophyll fluorescence—a practical guide. *Journal of Experimental Botany*, **51**, 659–668.

Medlyn BE (1998) Physiological basis of the light use efficiency model. *Tree Physiology*, **18**, 167–176.

Meroni M, Rossini M, Guanter L, Alonso L, Rascher U, Colombo R, Moreno J (2009) Remote sensing of solar-induced chlorophyll fluorescence: review of methods and applications. *Remote Sensing of Environment*, **113**, 2037–2051.

Middleton EM, Cheng YB, Hilker T, Black TA, Krishnan P, Coops NC, Huemmrich KF (2009) Linking foliage spectral responses to canopy-level ecosystem photosynthetic light-use efficiency at a Douglas-fir forest in Canada. *Canadian Journal of Remote Sensing*, **35**, 166–188.

Migliavacca M, Galvagno M, Cremonese E *et al.* (2011) Using digital repeat photography and eddy covariance data to model grassland phenology and photosynthetic CO2 uptake. *Agriculture and Forest Meteorology*, **151**, 1325–1337.

Miura T, Huete AR, Yoshioka H (2000) Evaluation of sensor calibration uncertainties on vegetation indices for MODIS. *IEEE Transactions on Geoscience and Remote Sensing*, **38**, 1399–1409.

Monteith JL (1972) Solar radiation and productivity in tropical ecosystems. *The Journal of Applied Ecology*, **9**, 747–766.

Monteith JL (1977) Climate and the efficiency of crop production in Britain. *Philosophical Transactions of the Royal Society of London*, **281**, 277–294.

Naumann JC, Young DR, Anderson JE (2007) Linking leaf chlorophyll fluorescence properties to physiological responses for detection of salt and drought stress in coastal plant species. *Physiologia Plantarum*, **131**, 422–433.

Niinemets Ü, Kull O (2001) Sensitivity of photosynthetic electron transport to photoinhibition in a temperate deciduous forest canopy: photosystem II center openness, non-radiative energy dissipation and excess irradiance under field conditions. *Tree Physiology*, **21**, 899–914.

Porcar-Castell A, Tyystjärvi E, Atherton J *et al.* (2014) Linking chlorophyll a fluorescence to photosynthesis for remote sensing applications: mechanisms and challenges. *Journal of Experimental Botany*, **65**, 4065–4095.

Prince SD, Goward SN (1995) Global primary production: a remote sensing approach. *Journal of Biogeography*, **22**, 815–835.

Rascher U, Liebig M, Luttge U (2000) Evaluation of instant light-response curves of chlorophyll fluorescence parameters obtained with a portable chlorophyll fluorometer on site in the field. *Plant Cell and Environment*, **23**, 1397–1405.

Rascher U, Agati G, Alonso L *et al.* (2009) CEFLES2: the remote sensing component to quantify photosynthetic efficiency from the leaf to the region by measuring sun-induced fluorescence in the oxygen absorption bands. *Biogeosciences Discuss*, **6**, 2217–2266.

Reichstein M, Falge E, Baldocchi D *et al.* (2005) On the separation of net ecosystem exchange into assimilation and ecosystem respiration: review and improved algorithm. *Global Change Biology*, **11**, 1424–1439.

Rohacek K, Soukupova J, Bartak M (2008) Chlorophyll fluorescence: a wonderful tool to study plant physiology and plant stress. In: *Plant Cell Compartments – Selected Topics*, pp. 41–104. Research Signpost, Kerala, India.

Rossini M, Meroni M, Migliavacca M *et al.* (2010) High resolution field spectroscopy measurements for estimating gross ecosystem production in a rice field. *Agricultural and Forest Meteorology*, **150**, 1283–1296.

Seaton GGR, Walker DA (1990) Chlorophyll fluorescence as a measure of photosynthetic carbon assimilation. *Proceedings of the Royal Society of London*, **242**, 29–35.

Turner DP, Ritts WD, Cohen WB *et al.* (2003) Scaling gross primary production (GPP) over boreal and deciduous forest landscapes in support of MODIS GPP product validation. *Remote Sensing of Environment*, **88**, 256–270.

Van der Tol C, Verhoef W, Rosema A (2009a) A model for chlorophyll fluorescence and photosynthesis at leaf scale. *Agricultural and Forest Meteorology*, **149**, 96–105.

Van der Tol C, Verhoef W, Timmermans J, Verhoef A, Su Z (2009b) An integrated model of soil-canopy spectral radiance observations, photosynthesis, fluorescence, temperature and energy balance. *Biogeosciences*, **6**, 3109–3129.

Van der Tol C, Berry JA, Campbell PKE, Rascher U (2014) Models of fluorescence and photosynthesis for interpreting measurements of solar-induced chlorophyll fluorescence. *Journal of Geophysical Research: Biogeosciences*, **119**, 2312–2327.

Verrelst J, Rivera PR, Van der Tol C, Magnani F, Mohammed G, Moreno J. (2015) Global sensitivity analysis of the SCOPE model: what drives simulated canopy-leaving sun-induced fluorescence? *Remote Sensing of Environment*, **166**, 8–21.

Williams M, Richardson AD, Reichstein M *et al*. (2009) Improving land surface models with FLUXNET data. *Biogeosciences*, **6**, 1341–1359.

Wittenberghe SV, Alonso L, Verrelst J *et al*. (2013) Upward and downward solar-induced chlorophyll fluorescence yield indices of four tree species as indicators of traffic pollution in Valencia. *Environmental Pollution*, **173**, 29–37.

Wittenberghe SV, Alonso L, Verrelst J, Moreno J, Samson R (2015) Bidirectional sun-induced chlorophyll fluorescence emission is influenced by leaf structure and light scattering properties-A bottom-up approach. *Remote Sensing of Environment*, **158**, 169–179.

Wohlfahrt G, Gu L (2015) The many meanings of gross photosynthesis and their implication for photosynthesis research from leaf to globe. *Plant, Cell and Environment*, **38**, 2500–2507.

Xu ZZ, Zhou GS, Wang YL, Han GX, Li YJ (2008) Changes in chlorophyll fluorescence in maize plants with imposed rapid dehydration at different leaf ages. *Journal of Plant Growth Regulation*, **27**, 83–92.

Yang X, Tang J, Mustard JF, Wu J, Zhao K, Serbin S, Lee JE (2015) Solar-induced chlorophyll fluorescence that correlates with canopy photosynthesis on diurnal and seasonal scales in a temperate deciduous forest. *Geophysical Research Letters*, **42**, 2977–2987.

Yang X, Tang J, Mustard JF *et al*. (2016) Seasonal variability of multiple leaf traits captured by leaf spectroscopy at two temperate deciduous forests. *Remote Sensing of Environment*, **179**, 1–12.

Yuan W, Liu S, Zhou G *et al*. (2007) Deriving a light use efficiency model from eddy covariance flux data for predicting daily gross primary production across biomes. *Agricultural and Forest Meteorology*, **143**, 189–207.

Zarco-Tejada PJ, Catalina A, González MR, Martín P (2013) Relationships between net photosynthesis and steady-state chlorophyll fluorescence retrieved from airborne hyperspectral imagery. *Remote Sensing of Environment*, **136**, 247–258.

Zhang Y, Guanter L, Berry JA *et al*. (2014) Estimation of vegetation photosynthetic capacity from space-based measurements of chlorophyll fluorescence for terrestrial biosphere models. *Global Change Biology*, **20**, 3727–3742.

Zhang Y, Guanter L, Berry JA, van der Tol C, Yang X, Tang J, Zhang Fangmin (2016) Model-based analysis of the relationship between sun-induced chlorophyll fluorescence and gross primary production for remote sensing applications. *Remote Sensing of Environment*, **187**, 145–155.

Zhao M, Running SW (2010) Drought-induced reduction in global terrestrial net primary production from 2000 through 2009. *Science*, **329**, 940–943.

Supporting Information

Additional Supporting Information may be found in the online version of this article:

Figure S1. The seasonal pattern of the correction coefficient (c) for $F_{s,}$ the black line is the mean reference line.